Ray-Tracing Acceleration Technique Employing Genetic Algorithm for Radio Propagation Prediction

Tetsuro IMAI
NTT DoCoMo, Inc.
NTT DoCoMo R&D Center, 3-5 Hikari-no-oka, Yokosuka-shi 239-8536 Japan
imait@nttdocomo.co.jp

1. Introduction

Up to now, in wireless communication systems such as cellular systems and wireless LANs, it has been essential to predict the radio propagation loss when designing service areas. Furthermore, in order to estimate the performance of spatial-temporal signal processing techniques in practical communication environments, predicting propagation path characteristics such as the direction of arrival (DOA), direction of departure (DOD), and time of arrival (TOA) is important [1, 2]. The ray-tracing method is very attractive because several radio propagation characteristics can be simply predicted.

In the ray-tracing method, there is a tradeoff relationship between the prediction accuracy and computation time. In order to obtain a high level of prediction accuracy, it is necessary to trace the higher-order rays that undergo interaction (reflection, diffraction, or transmission) many times, while taking into account as many structures in a wide area as possible. Therefore, the number of ray-tracing processes increases and the amount of time increases. Many acceleration (and/or efficiency) techniques for ray-tracing processing were investigated [3-8].

In Section 2, a ray-tracing method is introduced that employs the genetic algorithm (or GA) to accelerate the ray-tracing processing [12-15]. Hereafter, we call this method the GA_RT method. Section 3 presents the performance of the GA_RT method based on numerical simulation results. Finally, the concluding remarks are given in Section 4.

2. Ray-Tracing Employing GA

2.1 Basic model

The GA_RT method is based on the imaging method as a ray-tracing method [11]. In the imaging method, the procedure for ray-tracing is described below.

1) Establish ray-paths while considering a combination of components (planes and wedges) that are extracted from structures in the computation area as shown in Fig. 1.
2) Search for interaction points for each path.
3) Confirm whether or not a ray can be traced for each path.

When the number of components is M and the number of interactions for the target ray is N, the number of combinations or ray-paths is expressed as N_{all} (= M^N). Therefore, the computation time nonlinearly increases with the number of structures for N>1. On the other hand, many paths are rejected in general in Step 3 because interaction points cannot be defined based on the components. Such eventually rejected paths however, cannot be known in advance. This means that the computation efficiency of the imaging method is low. In the proposed GA_RT method, the number of ray-paths is limited appropriately by using the GA in advance and the efficiency level increases as a result.

In the GA, a chromosome is defined as a combination of multiple genes, the corresponding characters of which are different from each other, and an individual is expressed by a chromosome [9, 10]. On the other hand, in the imaging method, ray-paths are expressed as combinations of components. This suggests that the GA has a high affinity to the imaging method when each ray-path is handled as an "individual." Figure 2 shows a population model for the GA_RT method. A component, a combination of components, and a ray-path are considered as a gene, chromosome, and individual, respectively. Note that population size $N_c << N_{all}$. In addition, the "fitness" of each individual is defined as the received power of a traced ray along the corresponding path. The processing procedure in the GA_RT method is described below.

1) Establish the initial path-group by randomly extracting N_c paths from the theoretically possible N_{all} ray-paths.
1') Reestablish the path-group by performing "selection," "crossover," and "mutation."
2) Trace the ray and calculate the received power as the fitness for each ray-path.
3) Evaluate the fitness for each ray-path.
4) Repeat Steps 1' through 4 until the finish condition is satisfied.

Here, in Steps 1 and 1', the path-group must be established (or reestablished) using the rules below.

- A ray-path that repeats interaction continuously in the same component is not considered.
- Combinations of ray-paths must be different from each other in the path-group.

In this paper, the calculation rate, ρ, is defined as an indicator to estimate the finish condition, and is given by $\rho = \frac{1}{N_{all}} \sum_i N_{cal}^{(i)}$, where $N_{cal}^{(i)}$ is the number of ray-paths that appear in the i^{th} generation (or iteration process), but the paths that have already appeared in previous generations are not counted. Ray-tracing is completed when the value of ρ exceeds the threshold value, ρ_{th} ($0 \le \rho_{th} \le 1$), which is determined before processing. This means that ray-tracing processing in the case of $\rho_{th} = 1$ is equal to the conventional imaging method and the computation efficiency is evaluated ρ times in the case of $\rho < 1$ in this paper even though the amount of time for the re-setting process that is performed based on the GA must be considered, strictly speaking.

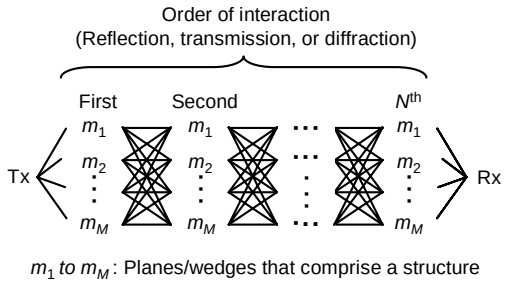

Figure 1: Ray-paths established based on combination of planes and wedges for imaging method.

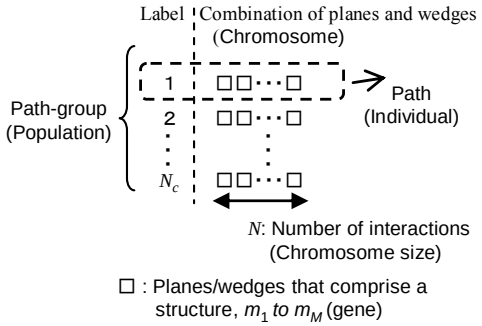

Figure 2: Population model.

2.2 Chain model

The purpose of the chain model is to perform the GA_RT method efficiently when there are many calculation points arranged on a surface, i.e., area prediction. The performance of the GA depends on the initial population. When the initial population is suitable, the optimal results can be obtained in a short time. However, it is generally difficult to know such population in advance.

Let us consider the case of performing ray-tracing with the conventional imaging method for two calculation points, *A* and *B*. The finally obtained ray-paths on *A* and *B* are different from each other when the location of *A* is far from that of *B*. However, as the locations approach each other, the difference becomes smaller. This means that when the calculation for *A* was already finished, the finally obtained ray-paths on *A* become suitable as the initial path-group on *B*. Based on this idea, the chain model is proposed as shown in Fig. 3.

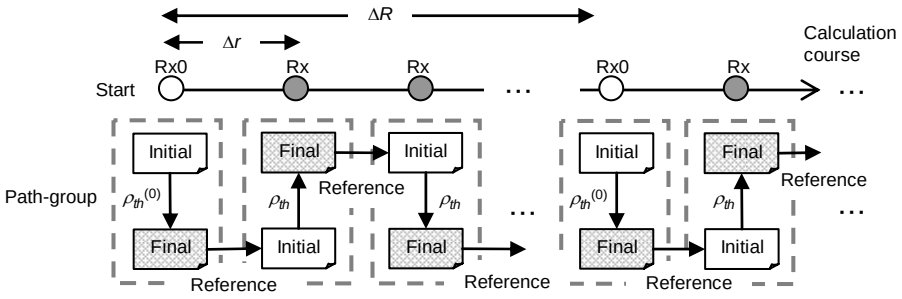

Figure 3: Chain model

In the chain model, first, the calculation order is established so that the distance, Δr, between calculation points becomes as short as possible. This process is called "course setting." Next, the following two kinds of calculation points are defined.

- Initial point, Rx0: the initial path-group is established randomly.
- Normal point, Rx: the initial path-group is established by referring to that of the previous point.

Here, ΔR ($\geq \Delta r$) as shown in Fig. 3 is the distance between the initial points. As a special case, all calculation points become initial points for $\Delta R = \Delta r$ and become normal points for $\Delta R = \infty$, except for the start point. Terms $\rho_{th}^{(0)}$ and ρ_{th} are threshold values for the calculation rate, which is established in the steps for Rx0 and Rx, respectively.

3. Performance Evaluation

In this section, the GA_RT method is evaluated through comparison with the conventional imaging method. Thus, the computational efficiency and accuracy are evaluated using the above mentioned calculation rate and calculation error of the received power, respectively. Here, calculation error is defined as the ratio of received power for the GA_RT method to that for the imaging method.

In Fig. 4, we show the numerical simulation results. Here, a two-dimensional model in the horizontal plane, in which the walls have two vertical edges are randomly distributed in a 2 km$\times$ 2 km area, is used as the calculation model. The location of Tx is (0, -500). The calculation points are set on a meandering course with the start point at (−1000, −1000) and the end point at (1000, 1000) in the 2 km$\times$ 2 km area. Since distance Δr is set to 10 m, the number of calculation points is 40,401. Furthermore, all points except for the start point are normal points because $\Delta R = \infty$. Table 1 gives the calculation conditions. Figures 4(a), 4(b), and 4(c) are the calculated received power distributions of the conventional imaging method (which is defined as the true result in this paper), the GA_RT method without the chain model (ρ_{th} = 0.2), and the GA_RT method with the chain model ($\rho_{th}^{(0)}$ = 0.5, ρ_{th} = 0.05), respectively. In these figures, the short red line segments represent the distributed walls. These results clearly show that the GA_RT method with the chain model is very effective for area prediction. The cumulative probability of the calculation error calculated from the results of Figs. 4(a)-4(c) are shown in Fig. 4(d). The computation time is minimized to approximately 6% by using the GA_RT method with the chain model, when a cumulative 50% value of the absolute error of less than 1 dB (mean vale is approximately 1 dB) is acceptable.

Table 1: Calculation Conditions

Structure	Material quality	Concrete (e_r = 6.76, s = 0.0023)
	Width, thickness	30, 0 m
	Number of structures: M_0, Total no. of planes and wedges: M	10 to 300, M (= $3M_0$) = 30 to 900
Ray-tracing	Frequency	2 GHz
	Number of reflections and diffractions: N	2
	Max. number of transmissions, transmission loss	∞, 10 dB
Genetic algorithm	Path-group size: N_c	Min (2MN, 100)
	Selection	Elitist strategy
	Crossover	Single-point crossover
	Mutation probability: P_m	0.01

4. Conclusions

In order to minimize the computation time while maintaining a high level of calculation (or prediction) accuracy, we introduced the GA_RT method with the chain model as a ray-tracing acceleration technique. The GA_RT method effectively applies the GA to ray-tracing processing based on the imaging method, and the chain model supports the GA_RT method efficiently when there are many calculation points arranged on a surface, i.e., area prediction. Furthermore, the effectiveness of the method was simulated numerically, and the results showed that a reduction in the computation time by a factor of approximately 17 times is achieved if an error rate of approximately 1 dB is acceptable. Note that this was evaluated based on a comparison with the conventional imaging method.

The GA_RT method can also be used in combination with other optimization methods. We have already completed an implementation of a previously developed practical propagation prediction system called 3D-PRISM (Three-Dimensional Propagation prediction with Ray-tracing Intelligent web-Shared system for Mobile radio) [16]. The next task is to perform a parameter study

to make the GA_RT method work effectively with 3D-PRISM and verify the prediction results of the 3D-PRISM-GA_RT combination through comparison with the measurement results.

References

[1] A. Paulraj and B. C. Ng, IEEE Personal Communications, pp. 36-48, Feb. 1998.
[2] R. B. Ertel, et al., IEEE Personal Communications, pp. 10-22, Feb. 1998.
[3] G. Liang and H. L. Bertoni, IEEE Trans. AP, Vol. 46, No. 6, pp. 853-863, June 1998.
[4] J. Rossi and Y. Gabillet, IEEE Trans. AP, Vol. 50, No. 4, pp. 517-523, April 2002.
[5] F. Agelet, et al., IEEE Trans. VT, Vol. 49, No. 6, pp. 2089-2104, Nov. 2000.
[6] Z. Yun, Z. Zhang, and M. Iskander, IEEE Trans. AP, Vol. 50, No. 5, pp. 750-758, May 2002.
[7] T. Imai and T. Fujii, AP2000, 2000.
[8] T. Imai, et al., NTT DoCoMo Technical Journal, Vol. 6, No. 1, pp. 41-51, June 2004.
[9] M. Mitchell, AN INTRODUCTION TO GENETIC ALGORITHMS, Tokyo Denki University Press 1996. (In Japanese)
[10] Y. Rahmat-Samii and E. Michielssen, Electromagnetic Optimization by Genetic Algorithms, John Wiley & Sons, Inc. 1999.
[11] T. Sarkar et al., IEEE AP Magazine, Vol. 45, No. 3, pp. 51-82. June 2003.
[12] T. Imai, IEICE Trans. (B), Vol. J89-B, No. 4, pp. 560–575, Apr. 2006 (in Japanese).
[13] T. Imai, EuCAP2006, 2006.
[14] T. Imai, NTT DoCoMo Technical Journal, Vol. 9, No. 3, pp. 20-27, Dec. 2007.
[15] T. Imai, NTT Technical Review, Vol. 6, No. 2, pp. 1-9, Feb. 2008.
[16] J. Mizuno, et al., IEICE technical report, AP 2007-136, pp. 81-86, Jan. 2008. (In Japanese)

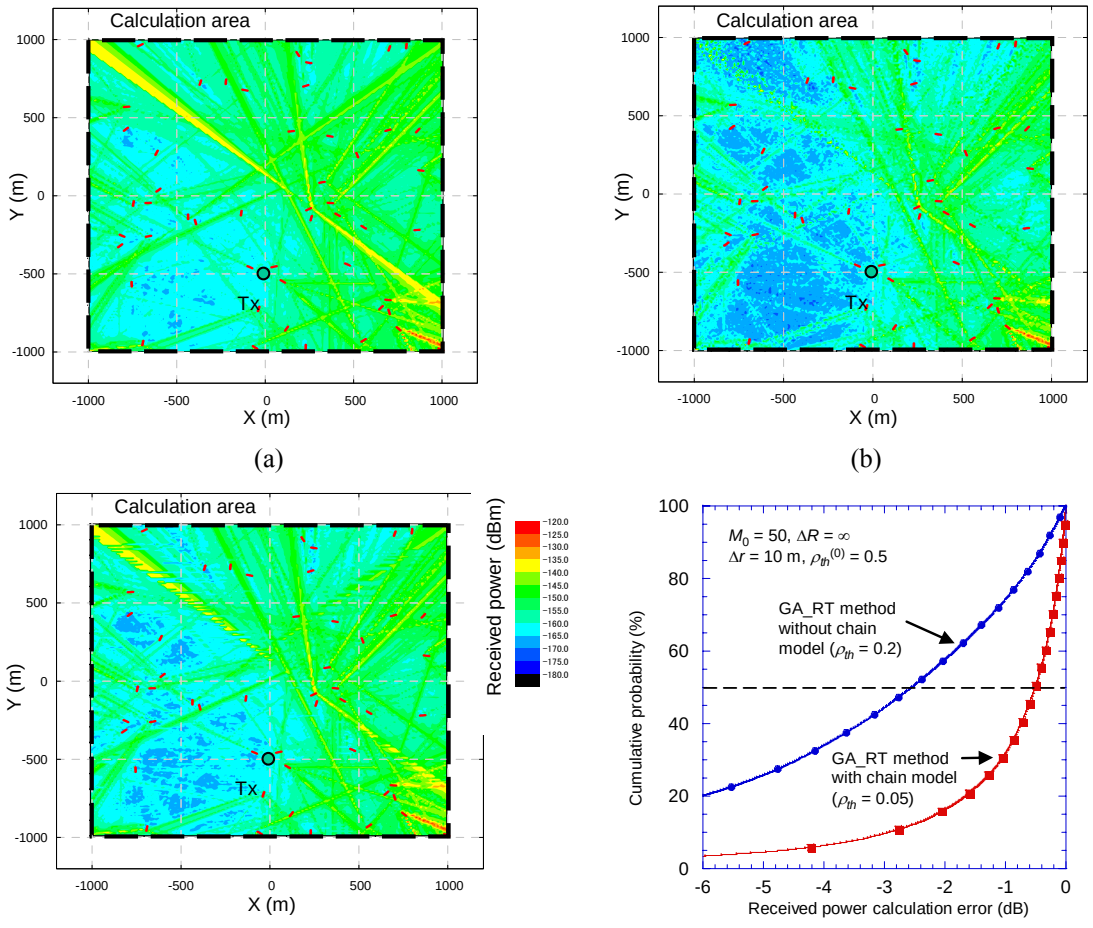

Figure 4: Numerical simulation results. (a) Received power distributions of conventional ray-tracing method using imaging method, (b) that of GA_RT method without Chain model, (c) that of GA_RT method with Chain model, (d) cumulative probability of calculation error in the GA_RT method with and without Chain model.